iScience, Volume *26*

Supplemental information

Tumor-suppressive role of the *musculoaponeurotic fibrosarcoma* gene in colorectal cancer

Hiroaki Itakura, Tsuyoshi Hata, Daisuke Okuzaki, Koki Takeda, Kenji Iso, Yamin Qian, Yoshihiro Morimoto, Tomohiro Adachi, Haruka Hirose, Yuhki Yokoyama, Takayuki Ogino, Norikatsu Miyoshi, Hidekazu Takahashi, Mamoru Uemura, Tsunekazu Mizushima, Takao Hinoi, Masaki Mori, Yuichiro Doki, Hidetoshi Eguchi, and Hirofumi Yamamoto

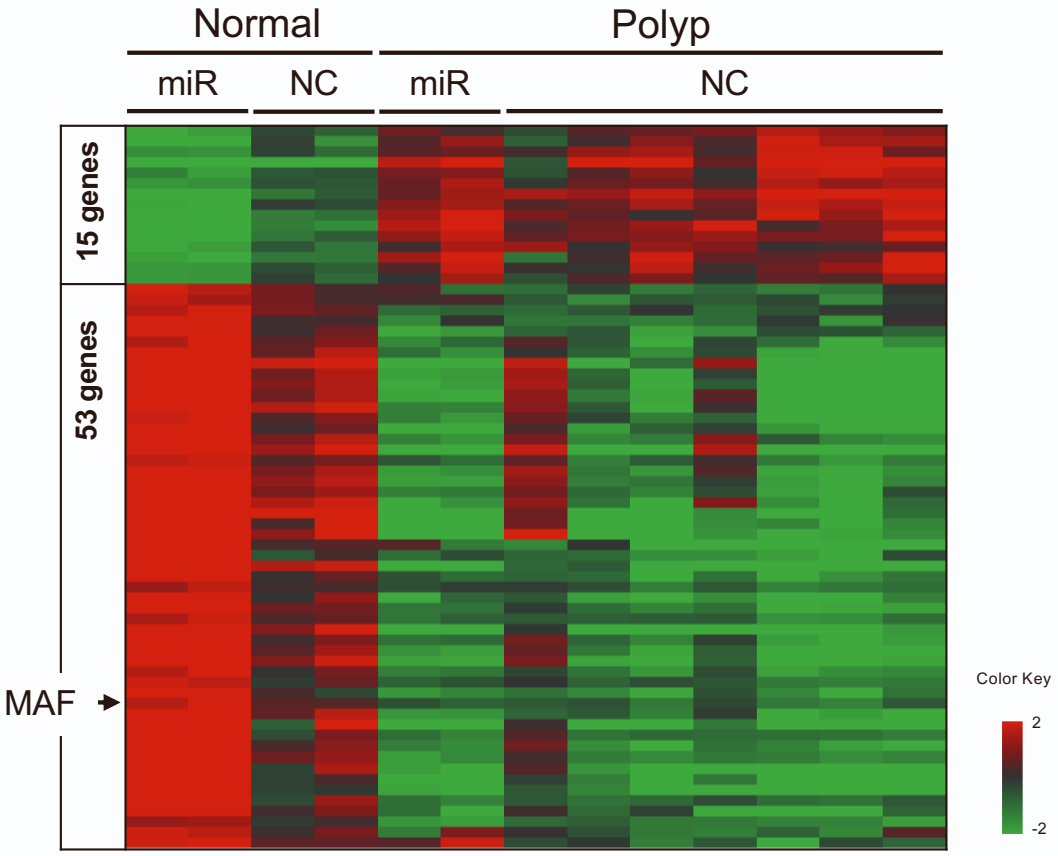

Figure S1. Heat map analysis of normal mucosa and polyps in *CpC;Apc* mice treated with the mouse miR cocktail (miRs: 200c, 302a-d, 369) or with negative control (NC) miRNA, related to Figure 1 A subset of normal mucosa and polyps with RIN (RNA integrity number) >6.3 were subject to microarray analysis (Normal-miRs; n = 2, Normal NC; n = 2, polyp miRs; n=2, polyp NC; n = 7).

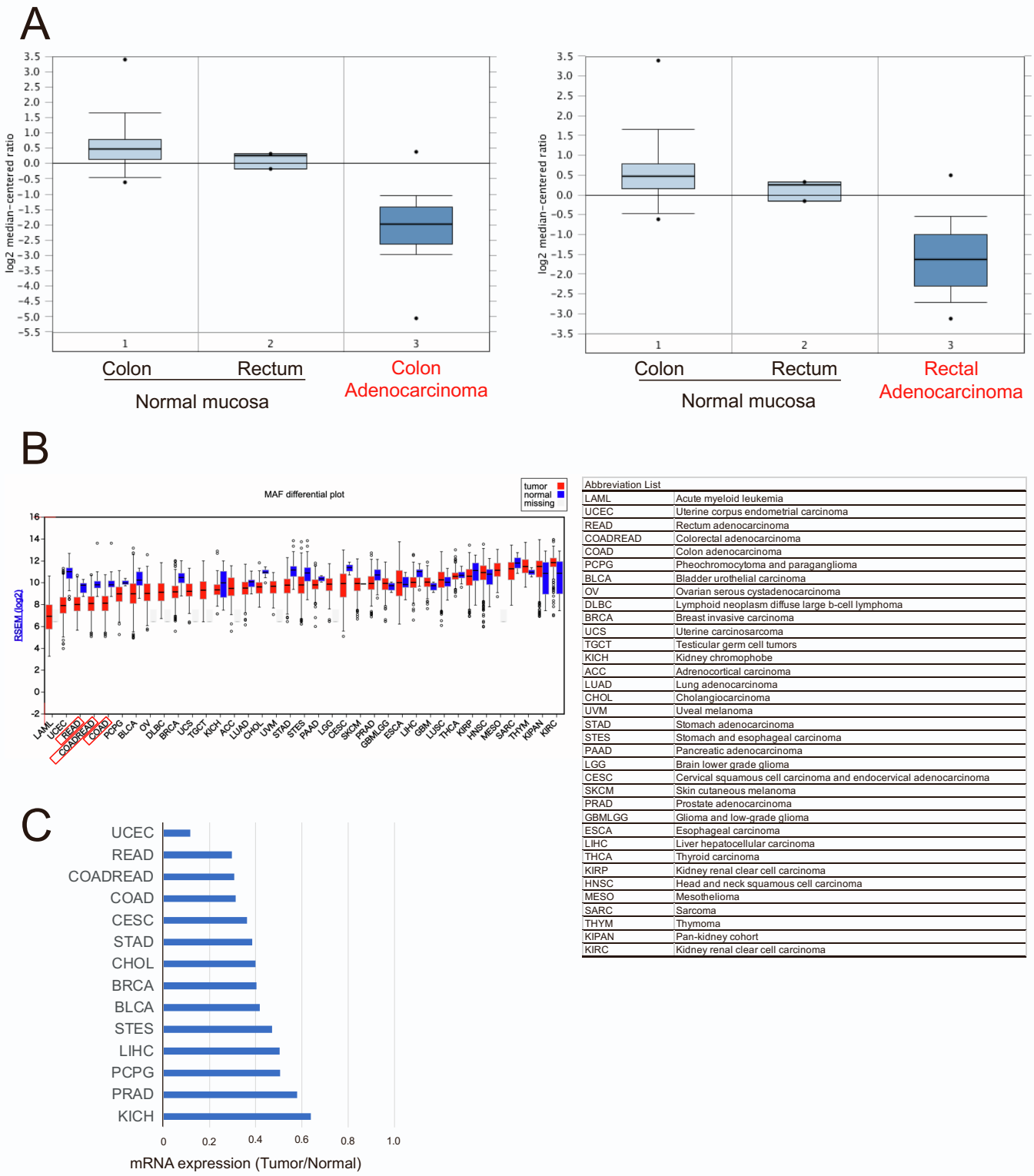

Abbreviation List	
LAML	Acute myeloid leukemia
UCEC	Uterine corpus endometrial carcinoma
READ	Rectum adenocarcinoma
COADREAD	Colorectal adenocarcinoma
COAD	Colon adenocarcinoma
PCPG	Pheochromocytoma and paraganglioma
BLCA	Bladder urothelial carcinoma
OV	Ovarian serous cystadenocarcinoma
DLBC	Lymphoid neoplasm diffuse large b-cell lymphoma
BRCA	Breast invasive carcinoma
UCS	Uterine carcinosarcoma
TGCT	Testicular germ cell tumors
KICH	Kidney chromophobe
ACC	Adrenocortical carcinoma
LUAD	Lung adenocarcinoma
CHOL	Cholangiocarcinoma
UVM	Uveal melanoma
STAD	Stomach adenocarcinoma
STES	Stomach and esophageal carcinoma
PAAD	Pancreatic adenocarcinoma
LGG	Brain lower grade glioma
CESC	Cervical squamous cell carcinoma and endocervical adenocarcinoma
SKCM	Skin cutaneous melanoma
PRAD	Prostate adenocarcinoma
GBMLGG	Glioma and low-grade glioma
ESCA	Esophageal carcinoma
LIHC	Liver hepatocellular carcinoma
THCA	Thyroid carcinoma
KIRP	Kidney renal clear cell carcinoma
HNSC	Head and neck squamous cell carcinoma
MESO	Mesothelioma
SARC	Sarcoma
THYM	Thymoma
KIPAN	Pan-kidney cohort
KIRC	Kidney renal clear cell carcinoma

Figure S2. Database survey of c-MAF mRNA expression in human cancers, related to Figure 1 (A) c-MAF mRNA level decreased in colon and rectum. The public database ONCOMINE™ indicated that c-MAF mRNA expression was decreased in adenocarcinoma of colon and rectum compared with normal mucosa. Data are expressed as median ± standard deviation.(B) Comparison of c-MAF mRNA expression between tumor and normal tissues in a series of human malignancies (http://firebrowse.org/). Data are expressed as the median and interquartile range (IQR) (C) Many human malignancies, including colon (COAD) and rectal cancer (READ) or both (COADREAD) expressed lower levels of c-MAF mRNA as compared with their normal counterparts.

A

Type		Sangar sequence (5' to 3')
Wild type		GCTGGCCACCCAGCACAGCCCGCTGGCCCCTGTCCTGCAGCCCATCTGGCGGAGCGGCGGC GGCGGTGGCGGCGGAGGCAGGAGGATGGCTTCAGAACTGGCAATGAACAATTCCGACCTGC CCACCAGTCCCCTGGCCATGGAATATGTTAATGACTTCGATCTGATGAAGTTTGAAGTGAAAAA GGAACCGGTGGAGACCGACCGCATCATCAGCCAGTGCGGCCGTCTCATCGCCGGGGGCTCG CTGTCCTCCACCCCCATGAGCACGCCCTGCAGCTCGGTGCCCCCNTCNNNCANGNTNNNNNNN NNNNNNNNNN
1 nucleotide deletion	homo	NNNTGTGCACGTTCGAGCTTTCGGGCCACAGCCACCGCCGCGCAAGCTAGAAGCGCCCTAGC CCGGCAAGCTGGCTCACCCGCTGGCCACCCAGCACAGCCCGCTGGCCCCTCTCCTGCAGCCC ATCTGGCGGAGCGGCGGCGGCGGTGGCGGCGGAGGCAGGAGGATGGCTTCA-AACTGGCAA TGAACAATTCCGACCTGCCCACCAGTCCCCTGGCCATGGAATATGTTAATGACTTCGATCTGAT GAAGTTTGAAGTGAAAAAGGAACCGGTGGAGACCGACCGCATCATCAGCCAGTGCGGCCGTCT CATCGCCGGGGGCTNNNNNNCCTCCACCCCCATGAGCACGCCCTGCAGCTCGGTGCCCCCNT CCCCCAGCNNCTNGGNNNNNNNNNNN
	hetero	NNNNNNNNNNNNTNNNNNNNTNGGGNCNNNNNCCNCNNNNNNCCANNNNNNANNNNCNNNNN CCNGNNANNNNGNNNNNCCNNNNGNCCNNCNNNNNNNNNCCNNNGGNCCCTTTTNNNNNNNCC NTTNNGNNGNNNNGNNGNGGNNGNNGNNGNNGNNGCCNGNNGNNNGNNTTNNAACTGGCAA TGAACAATTCCGACCTGCCCACCAGTCCCCTGGCCATGGAATATGTTAATGACTTCGATCTGAT GAAGTTTGAAGTGAAAAAGGAACCGGTGGAGACCGACCGCATCATCAGCCAGTGCGGCCGTCT CATCGCCGGGGGCTCGCTGTCCTCCACCCCCATGAGCACGCCCTGCAGCTCGGTGCCCCCNT CCCCCAGCTCTNGGCNCCNNNNNNN
8 nucleotide deletion	homo	NGTGTGCACGTTCGAGCTTTCGGGCCACAGCCACCGCCGCGCAAGCTAGAAGCGCCCTAGCC CGGCAAGCTGGCTCACCCGCTGGCCACCCAGCACAGCCCGCTGGCCCCTCTCCTGCAGCCCA TCTGGCGGAGCGGCGGCGGCGGTGGCGGCGGAGGCAGGAGGATGGCT--------GGCAATGAA CAATTCCGACCTGCCCACCAGTCCCCTGGCCATGGAATATGTTAATGACTTCGATCTGATGAAG TTTGAAGTGAAAAAGGAACCGGTGGAGACCGACCGCATCATCAGCCAGTGCGGCCGTCTCATC GCCGGGGGCNNNNNNNTCCTCCACCCCCATGAGCACGCCCTGCAGCTCGGTGCCCCCNTCCCC CAGCTCTNGGCNNNCNNNN
	hetero	TGTGTGCNTGTGTGCACNTTCGAGCCTCAGGCCCCCACGCGCAAGCGAGCAAGCTAGAAGCC CGGCAAGCTGGCTAGCTGGCTCACCCGCCGGCCCACCAGCACAGCCCGTTTCCCCCTGTCCA TCAGGCCGTGCGGCCGGAGCGGGGGGGGCGGGGGGCCAGGGGGACAGGATGAGGGCTGGCA ATGAACAATTCCGACCTGCCCACCAGTCCCCTGGCCATGGAATATGTTAATGACTTCGATCTGA TGAAGTTTGAAGTGAAAAAGGAACCGGTGGAGACCGACCGCATCATCAGCCAGTGCGGCCGTC TCATCGCCGGGGGCTCGCTGTCCTCCACCCCCNATGAGCNCGCCCTGCTGCTCGGTGCCCCC GTCCCCCCAGCTCTCGGCNCCCNNNC

B

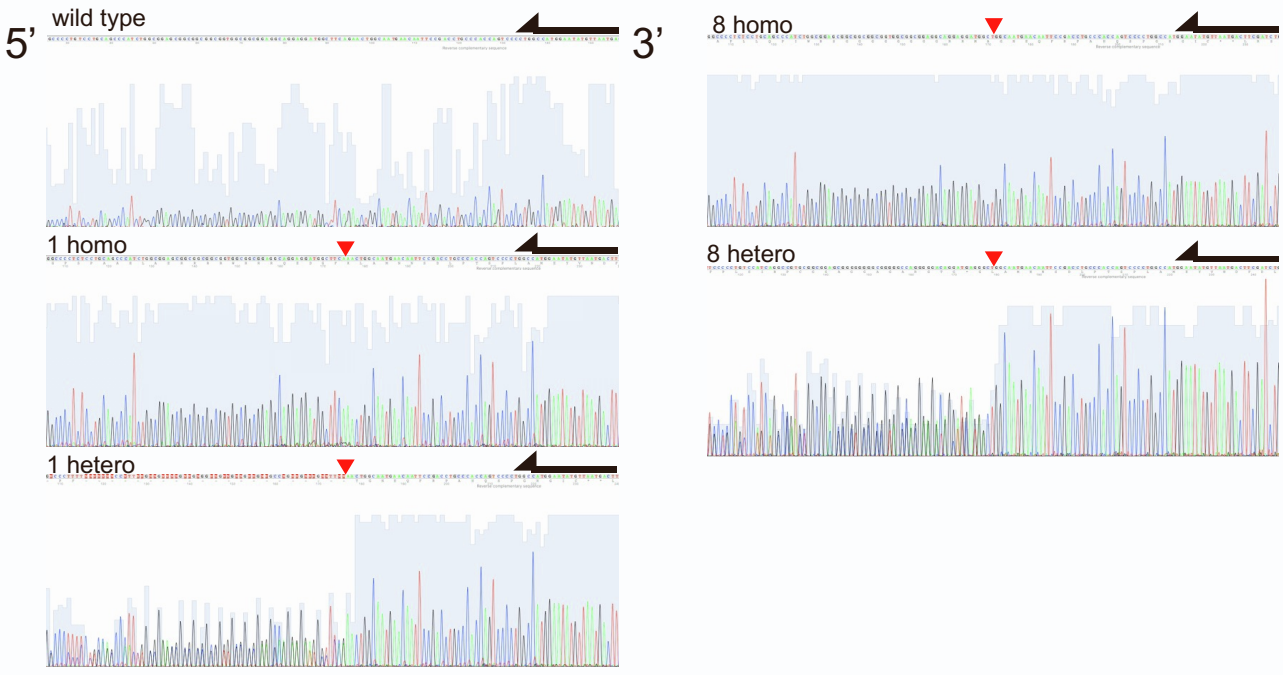

Figure S3. Genotyping of wild-type and *c-MAF* KO mice, related to Figure 5 (A) Base sequence for each type of knockout mice and wild type. Red arrowheads indicate the deletion start site viewed from the 3' side and deleted sequences are indicated by the dotted line. To clarify deletion sites in comparison with the wild-type sequence, the corresponding sequences were marked in blue, green, and red. (B) Chromatograms for each base deletion in knockout mice and for wild type. Red arrowheads indicate the deletion start site viewed from the 3' side. Black arrows on the right indicate read direction; note that heterogeneous KO region displays overlapped peaks on the 5' side from the red arrowhead while the homogeneous KO region showed a single peak.

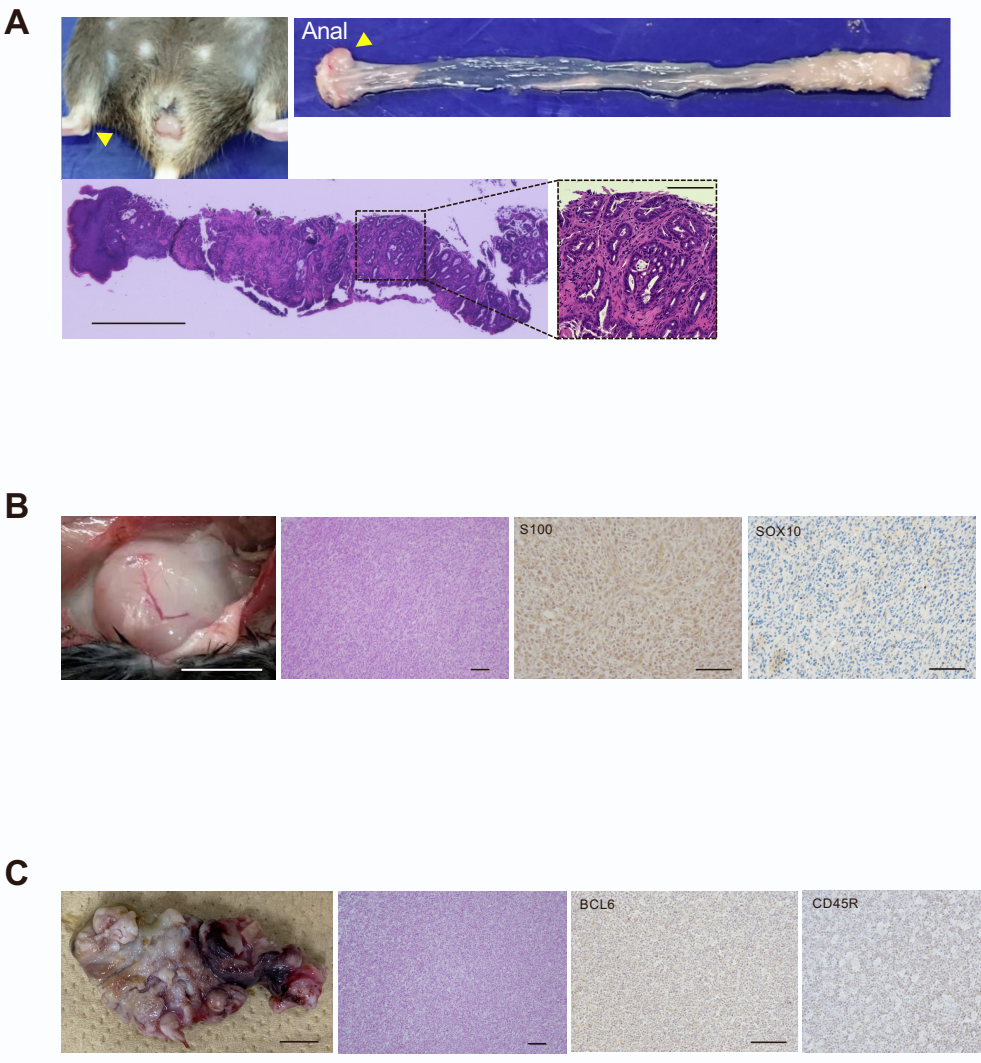

Figure S4. Spontaneous carcinogenesis in c-MAF KO mice, related to Figure 5 (A) One female mouse (8-nucleotide deletion/c-MAF hetero) had a prolapse of the bowel. Gross examination of the removed colorectum revealed that it was a rectal tumor. Histologically, it was a well- to moderately differentiated adenocarcinoma (scale bar: left; 700 mm, right; 150 mm). (B) In one male mouse (one-nucleotide deletion/c-MAF hetero), a pale white tumor was observed on the chest wall (scale bar: 1 cm). By H&E and immunohistochemical staining (S100-positive, SOX10-negative), the tumor was diagnosed as a schwannoma (scale bar: 100 mm). (C) In one female mouse (one-nucleotide deletion/c-MAF hetero), a tumor that tightly adhered to the small intestine was observed (scale bar: 1 cm). Through histological examination and immunohistochemical analysis, it was weakly BCL6 positive and CD45R positive and diagnosed as Burkitt's lymphoma (scale bar: 100 mm).

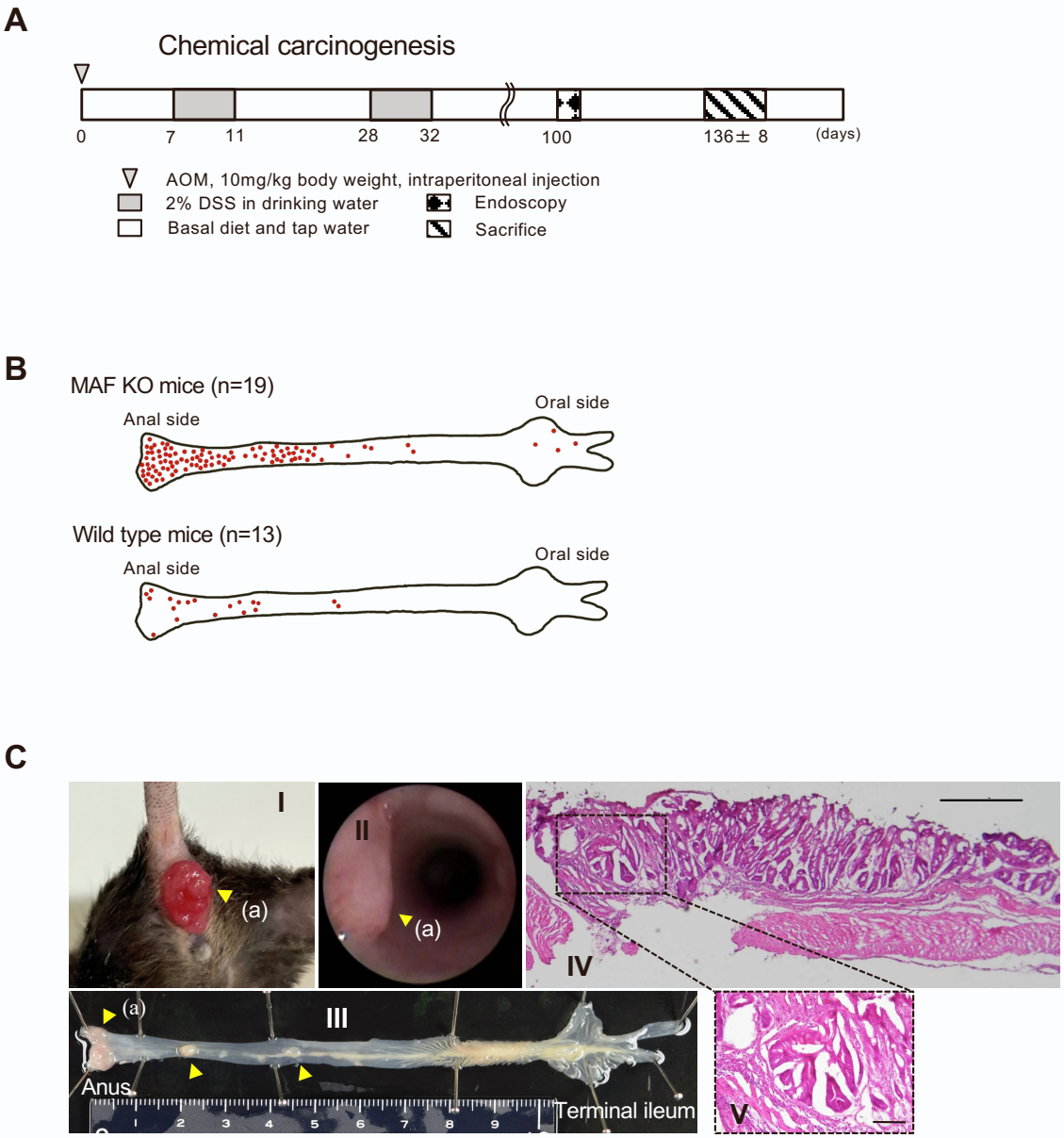

Figure S5. colitis-associated tumor formations in c-MAF knockout mice related to Figure 5 (A) Experiments protocol of chemical carcinogenesis. AOM was intraperitoneally injected on day 0, and 2% DSS was administered in drinking water on days 7–11 and 28–32. (B) The distribution of tumors in the colon. Each red dot indicates a tumor. (C) The finding of one c-Maf KO mouse. (I) On day 100, one mouse had a prolapse from the anus, indicated by the yellow arrowhead in (a). (II) Endoscopic examination confirmed it was rectal tumor (yellow arrowhead in (a)) and revealed that multiple tumors existed. (III) Gross findings of the removed colon and rectum. A rectal tumor indicated by the yellow arrowhead (a) and another two polyps (indicated by arrowheads) were noted. (IV) H&E staining of the rectal tumor. Histological diagnosis was well- to moderately differentiated adenocarcinoma. Scale bar: 500 mm. (V) Magnification view of the rectangle area. Scale bar: 100 mm. AOM, Azoxymethane; DSS, Dextran Sodium Sulfate; KO, knock out.

A

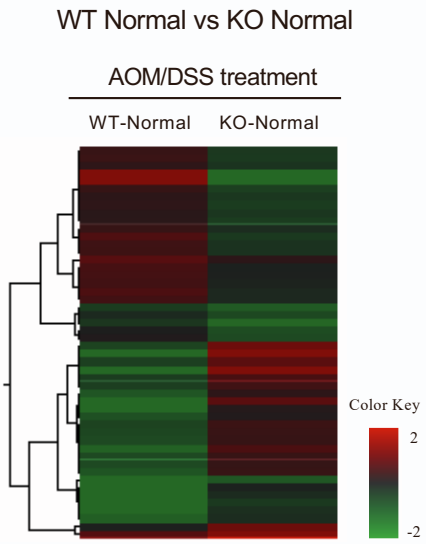

WT-Normal/KO-Normal
Up & Down Top 25

ID	Fold Change	*P* value
Xist	94.870	0.009
Hba-a2	58.735	0.043
Eif3j1	33.139	0.040
Adig	6.726	0.001
Itln1	6.578	0.033
Pnliprp2	6.041	0.013
Cpa2	5.731	0.042
Clps	3.942	0.008
Gsdmc	3.844	0.004
Duoxa1	3.763	0.003
Car3	3.693	0.027
S100a9	3.410	0.007
Tpsb2	3.379	0.007
Cryba4	3.368	0.010
Tuba8	3.160	0.004
Clca1	3.150	0.012
Gm13212	3.081	0.003
Ly6c2	3.062	0.021
Adgre4	3.029	0.028
Ear2	2.992	0.037
Tg	2.962	0.040
C130026I21Rik	2.879	0.003
Chst13	2.806	0.015
Gsdmcl-ps	2.648	0.021
Fpr2	2.617	0.007
Eif2s3y	0.013	0.012
Ddx3y	0.020	0.016
C330022C24Rik	0.331	0.024
Gm10768	0.367	0.030
Neat1	0.400	0.029
Fam19a3	0.418	0.013
Ddx60	0.446	0.004
Myom3	0.446	0.040
B430010I23Rik	0.447	0.029
Oasl2	0.451	0.028
Apoo-ps	0.453	0.038
Ccdc116	0.460	0.027
Gm3558	0.480	0.009
Apol9a	0.498	0.042
2410018L13Rik	0.527	0.032
Gm10069	0.535	0.031
Rhov	0.536	0.020
Ido1	0.543	0.003
4933430I17Rik	0.555	0.010
Vsig10l	0.560	0.049
BC051142	0.561	0.020
5031434O11Rik	0.561	0.026
Npb	0.571	0.050
Slc4a4	0.572	0.045
Ttc16	0.573	0.036

B

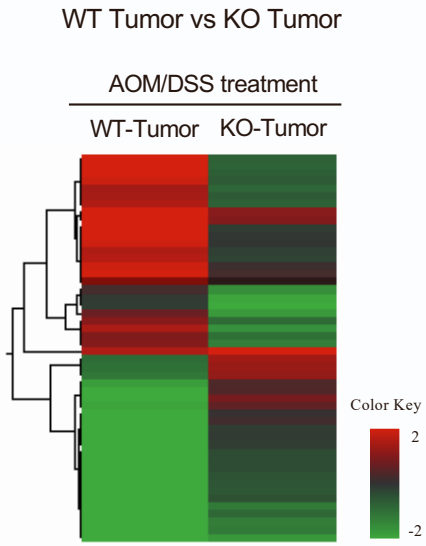

WT-Tumor/KO-Tumor
Up & Down Top 25

ID	Fold Change	*P* value
0610040F04Rik	11.850	0.003
Cbxn3	10.868	0.023
Mab21l2	7.133	0.018
Angptl7	6.820	0.029
Vip	6.722	0.031
B3gnt6	5.998	0.017
Hand2	5.646	0.004
Dmrta2	5.645	0.002
Prph	5.487	0.007
Gdf10	5.475	0.038
Sst	5.367	0.004
Matn4	5.241	0.005
H19	5.115	0.019
Fzd9	5.094	0.001
Mfap4	5.066	0.001
Fmod	4.873	0.005
Upp2	4.791	0.043
Snrpn	4.750	0.003
Kcnh3	4.702	0.007
Calb2	4.572	0.006
Acaa1b	4.470	0.007
Tmem59l	4.421	< 0.001
Nov	4.288	0.007
Pou2f3	4.261	0.001
Col8a2	4.197	0.033
Hoxd11	0.049	0.013
Hoxd10	0.073	0.017
Hoxd13	0.080	0.027
Mettl7a2	0.119	0.007
Atp12a	0.148	0.004
Cps1	0.178	0.022
Cyp2d12	0.184	0.001
Lix1	0.193	0.025
Gzmk	0.196	0.012
Efhb	0.204	0.001
S100g	0.206	0.001
Zp2	0.212	0.038
Klhl14	0.236	0.008
Adh6a	0.239	0.031
Abcg5	0.242	0.008
Slc15a1	0.256	< 0.001
Lrrn3	0.257	0.003
Timp4	0.258	0.022
Cyp2c68	0.265	0.002
Trpv3	0.274	< 0.001
Cyp2d9	0.277	0.002
Scnn1g	0.291	0.014
Tgm3	0.291	0.038
Ddx60	0.293	0.006
Abcg8	0.303	0.031

Figure S6. RNA sequencing of colorectal tissue samples of wild-type and *c-MAF KO* mice after treatment with AOM/DSS, related to Figure 5 (A) The heat map of upregulated or downregulated gene expression in normal colonic mucosa between *c-MAF* KO mice and wild-type (WT) mice. (B) Heat map of gene expression in tumors between *c-MAF* KO mice and WT mice. AOM, Azoxymethane; DSS, Dextran Sodium Sulfate; KO, knock out.

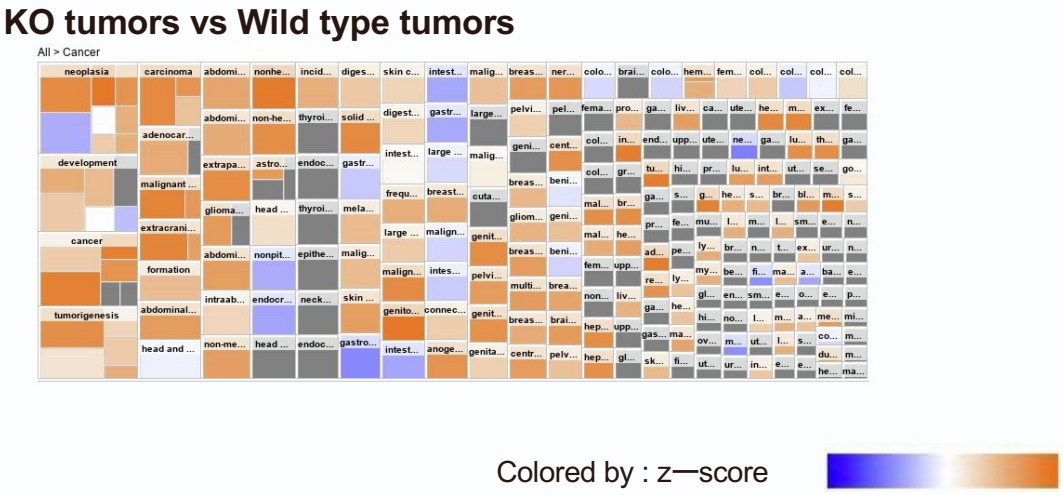

Figure S7. Ingenuity Pathway Analysis of downstream disease and function in tumors of *c-MAF* KO mice related to Figure 5 A number of cancer-related categories were activated in *c-MAF* KO tumors compared with wild-type tumors. KO, knock out.

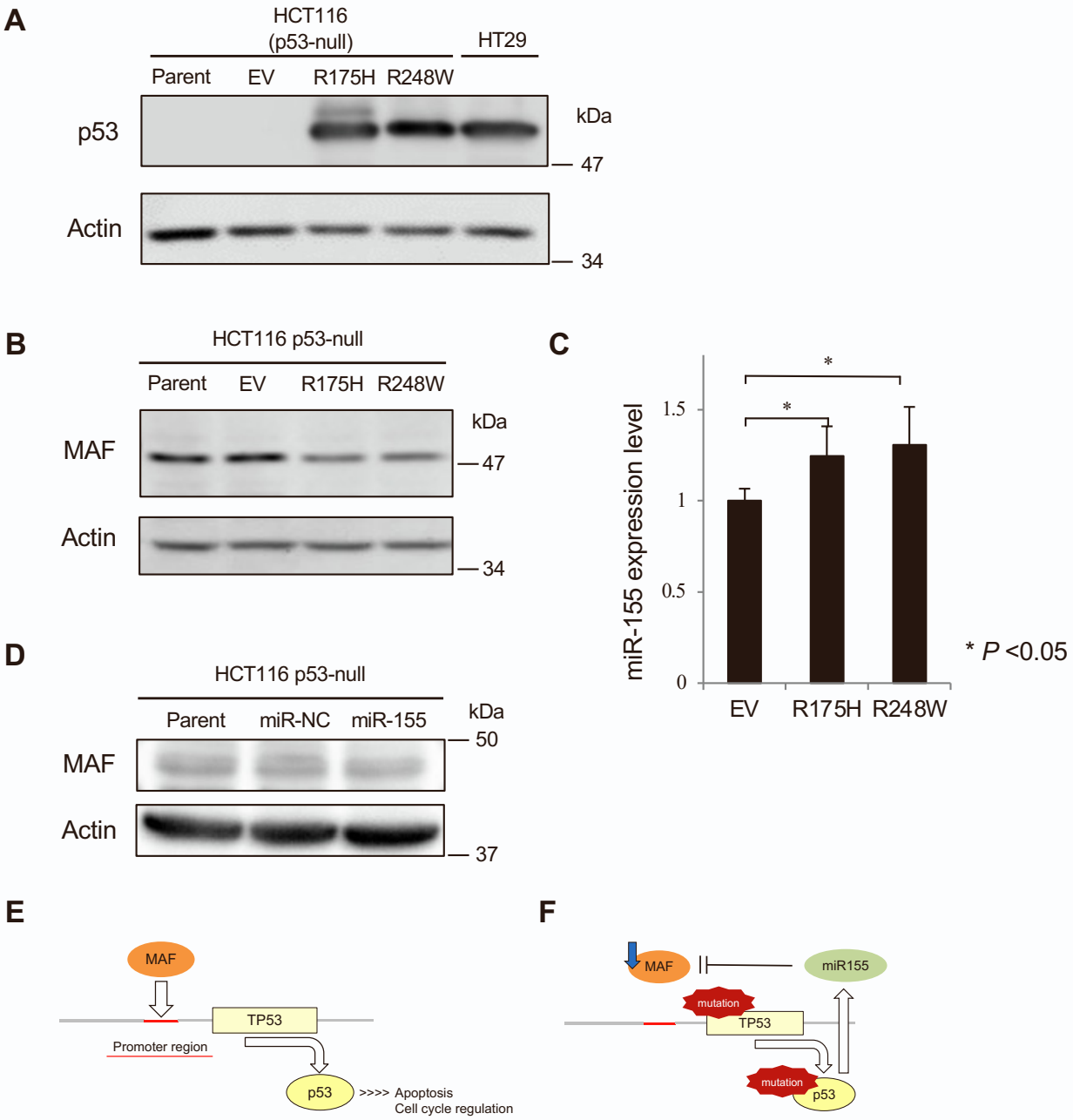

Figure S8. Effect on miR-155 induction of transduction of p53 mutation into p53-null HCT116 cells, related to Figure 6 (A) The mutated p53 plasmids (R175H, R248W) were transfected into p53-null HCT116 cells to produce p53 protein. The HT29 cells harboring the mutated p53 gene served as a positive control. Actin bands served as a loading control. (B) c-MAF expression was reduced in mutated p53-transfected cells. (C) qRT-PCR revealed that miR-155 levels significantly increased in mutated p53-transfected cells compared with vector control. (D) Expression of c-MAF was decreased in the miR-155–transfected cells. (E) The scheme of the relationship between c-MAF and p53 in normal mucosa. c-MAF acts as a transcription factor at the promoter region of TP53 and induces wild type p53 expression which regulates cell cycle and induces apoptosis. (F) The scheme of the relationship between p53 and c-MAF in p53 mutated tumors. Mutant p53 induces miR-155 which represses c-MAF expression. Data are expressed as mean ± standard deviation. EV: empty vector. *$P < 0.05$.

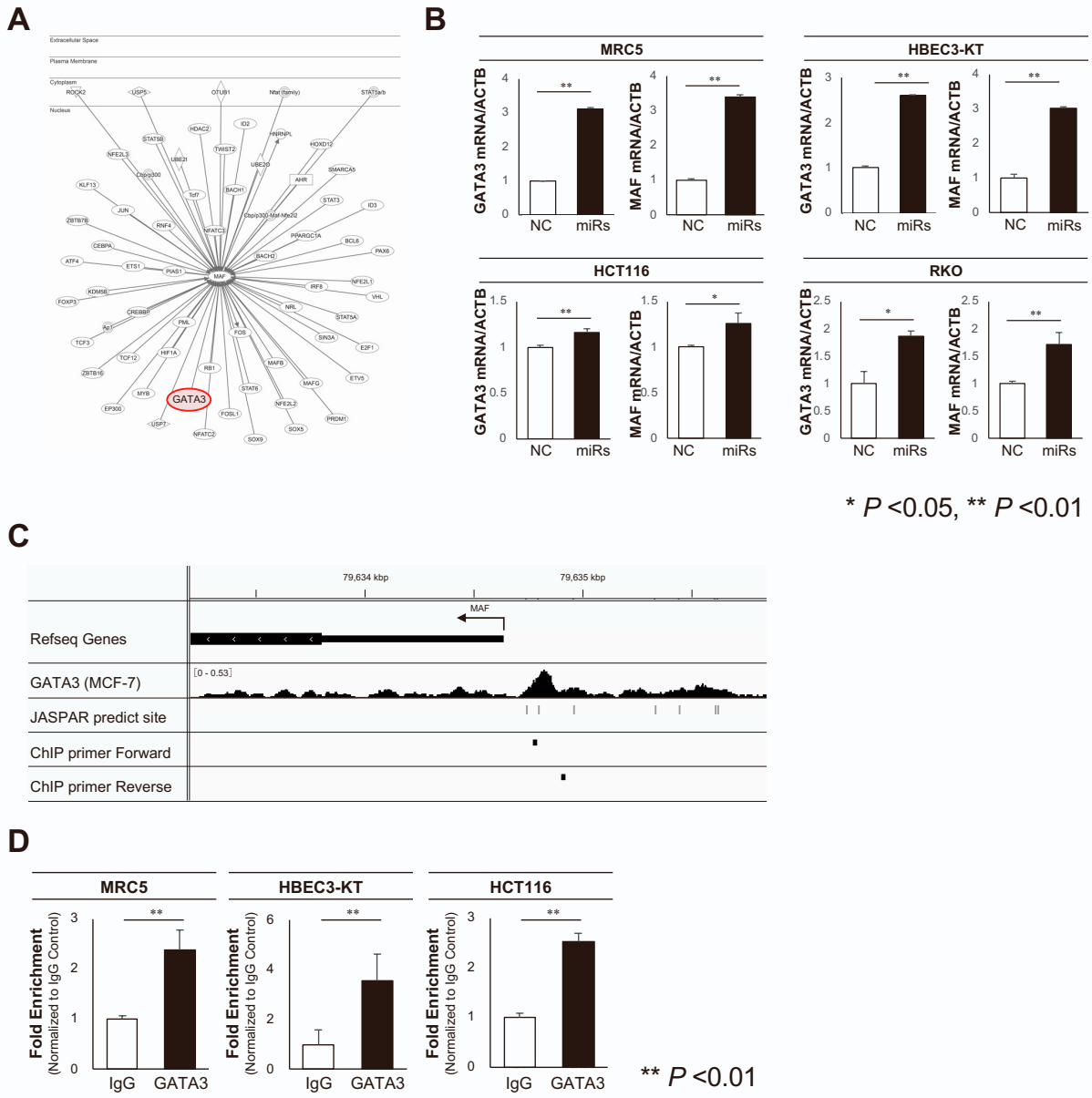

Figure S9. A candidate mechanism for how miRs-200c, -302a-d, and -369 induce c-MAF, related to Figure 1 (A) Ingenuity Pathway Analysis was used to create a gene relationship diagram centered on c-MAF. The diagram revealed that the transcription factor GATA3 positively regulates MAF expression, as previously reported [28]. (B) In MRC5 human lung fibroblasts, HBEC3-KT human bronchial epithelial cells and colorectal cancer cell lines (HCT116, RKO), treatment with the miRNAs increased GATA3 and c-MAF mRNA expression. (C) Integrative genome viewer (IGV) tracks of ChIP-seq peaks of GATA3 from the ChIP-Atlas database in MCF-7 cells, the predicted binding site for GATA3 by JASPAR database, and the positions of our designed primer. The ChIP-seq peaks of GATA3 was located before the transcription start site of c-MAF, and the predicted binding site from JASPAR was found in the range of the peak. The ChIP-PCR primer was designed in the range of peaks. (D) The binding of the GATA3 proteins to the c-MAF promoter in MRC5, HBEC3-KT and HCT116 cell lines analyzed by ChIP-qPCR. Fold enrichment normalized to the value of the IgG control is shown. Data are expressed as mean ± standard deviation. Statistical differences were analyzed using Student's *t* test. miRs, miRNAs. *$P < 0.05$, **$P < 0.01$.

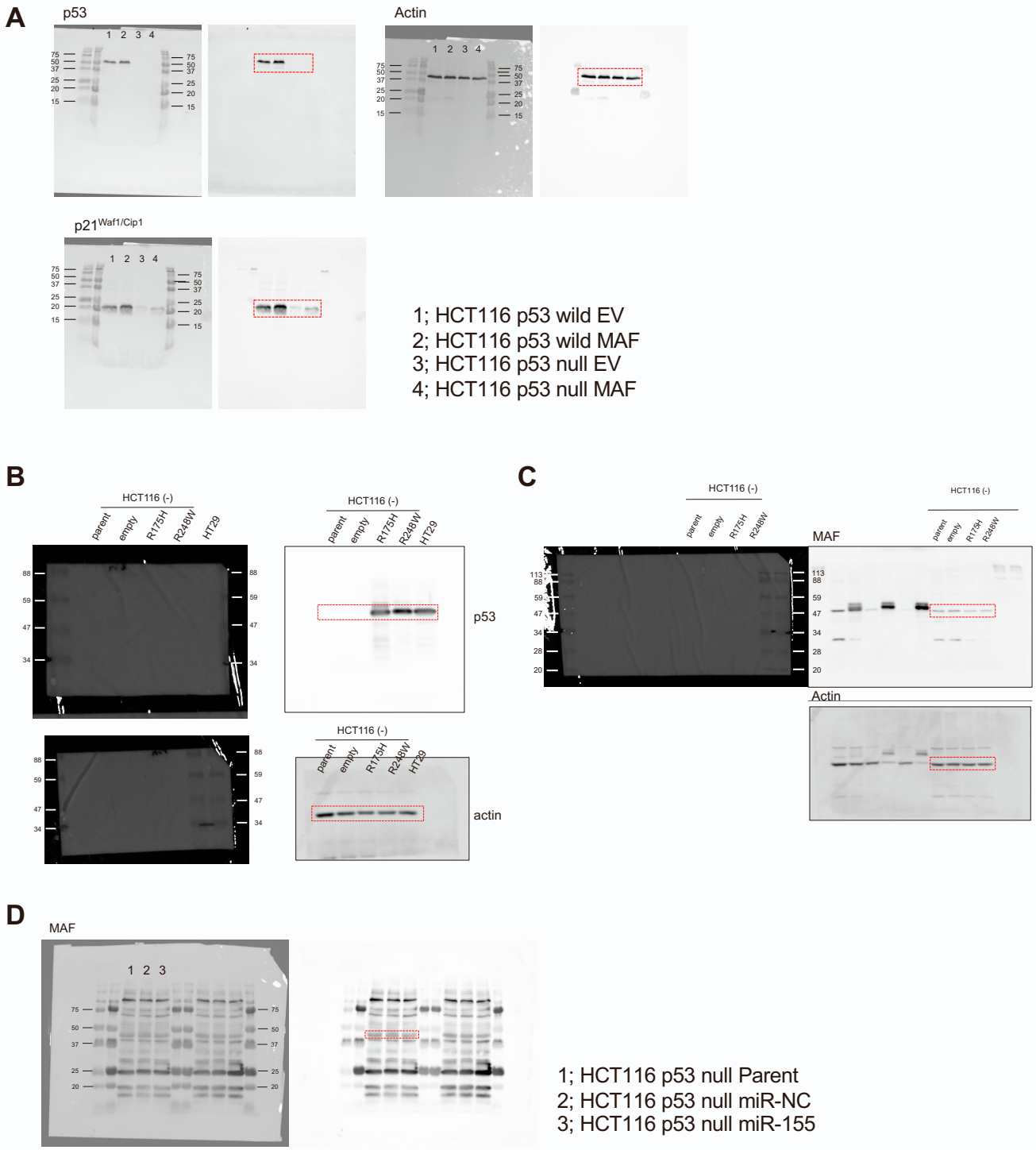

Figure S10. Western Blotting raw data, related to Figure 4 and S8

(A) The uncropped WB figures is for figure 4D. (B) The uncropped WB figures is for figure S8A. (C) The uncropped WB figures is for figure S8B. (D) The uncropped WB figures is for figure S8D.

Table S1. Sequences of miRNAs in human, mouse, and rat species, sense (5' to 3'), related to STAR Methods

	hsa (human)	mmu (mouse)	rno (rat)
miR-200c-3p	UAAUACUGCCGGGUAAUGAUGGA	UAAUACUGCCGGGUAAUGAUGGA	UAAUACUGCCGGGUAAUGAUG
miR-302a-3p	UAAGUGCUUCCAUGUUUUGGUGA	UAAGUGCUUCCAUGUUUUGGUGA	N/A
miR-302b-3p	UAAGUGCUUCCAUGUUUUAGUAG	UAAGUGCUUCCAUGUUUUAGUAG	N/A
miR-302c-3p	UAAGUGCUUCCAUGUUUCAGUGG	AAGUGCUUCCAUGUUUCAGUGG	N/A
miR-302d-3p	UAAGUGCUUCCAUGUUUGAGUGU	UAAGUGCUUCCAUGUUUGAGUGU	N/A
miR-369-3p	AAUAAUACAUGGUUGAUCUUU	AAUAAUACAUGGUUGAUCUUU	AAUAAUACAUGGUUGAUCUUU
miR-369-5p	AGAUCGACCGUGUUAUAUUCGC	AGAUCGACCGUGUUAUAUUCGC	AGAUCGACCGUGUUAUAUUCGC
miR-155	UUAAUGCUAAUCGUGAUAGGGGU		
Negative control	UAAAUGUACUGCGCGUGGAGAGGAA	UCACAACCUCCUAGAAAGAGUAGA	

Table S3. Relationship between c-MAF expression and clinical and pathological parameters, related to Figure 2

	Strong (n = 35)	Weak (n = 63)	*P* value
Age (years)			
≥ 65/< 65	17/18	35/28	0.507
Gender			
Male/Female	20/15	37/26	0.878
Location			
Rectum/Colon	11/24	32/31	0.064
Depth			
T4/Tis, T1, T2, T3[a]	2/33	7/56	0.375
Lymph node metastasis			
Negative/Positive	27/8	38/25	0.091
Histological type			
tub1, tub2/muc, por[b]	33/2	57/6	0.509
Lymphatic duct invasion			
Negative/Positive	17/18	12/51	0.002
Venous invasion			
Negative/Positive	27/8	39/24	0.123

a) Tis, carcinoma in situ; T1, involvement of submucosa; T2, involvement of muscularis propria; T3, involvement of subserosa; T4, involvement of serosal surface or direct invasion to other organs; b) tub1, well differentiated adenocarcinoma; tub2, moderately differentiated adenocarcinoma; muc, mucinous carcinoma; por, poorly differentiated adenocarcinoma

Table S4. Lists of Activated molecules in tumors of *c-MAF* KO mice compared with wild-type mice after treatment with AOM/DSS, related to Figure 5

Upstream Regulator	Molecule Type	Predicted Activation State	Activation z-score	*P* value
Vegf	**Growth factor**	**Activated**	**5.108**	**< 0.001**
IL4	**Cytokine**	**Activated**	**4.659**	**< 0.001**
IGF1	**Growth factor**	**Activated**	**4.581**	**< 0.001**
HGF	**Growth factor**	**Activated**	**4.57**	**< 0.001**
AGT	**Growth factor**	**Activated**	**4.527**	**< 0.001**
TRIM24	**Transcription regulator**	**Activated**	**4.484**	**< 0.001**
RNASEH2B	Other	Activated	4.413	< 0.001
JUN	**Transcription regulator**	**Activated**	**4.324**	**< 0.001**
TGFB1	**Growth factor**	**Activated**	**4.308**	**< 0.001**
EGF	**Growth factor**	**Activated**	**4.248**	**< 0.001**
Insulin	**Hormone**	**Activated**	**4.232**	**< 0.001**
SP1	Transcription regulator	Activated	4.102	< 0.001
NRG1	**Growth factor**	**Activated**	**4.041**	**0.001**
Ttc39aos1	Other	Activated	4.024	< 0.001
STAT3	**Transcription regulator**	**Activated**	**4.021**	**< 0.001**
CITED2	**Transcription regulator**	**Activated**	**4.02**	**< 0.001**
FGF2	**Growth factor**	**Activated**	**4.004**	**< 0.001**
NPM1	Transcription regulator	Activated	4	< 0.001
STAG2	Other	Activated	3.983	< 0.001
NKX2-3	**Transcription regulator**	**Activated**	**3.977**	**< 0.001**
PIK3CG	Kinase	Activated	3.965	< 0.001

Cancer-promoting growth factors, transcription factors, kinases, and cytokines are shown in bold.

Table S5. primer sequence (5' to 3') or TaqMan Gene Expression Assay ID for qRT-PCR, ChIP-PCR or generating *c-MAF* knock out mice, related to related to STAR Methods

Mus musculus	c-MAF		Mm02581355_s1
	Actb		Mm02619580_g1
Rattus norvegicus	c-MAF		Rn00824591_s1
	Actb		Rn00667869_m1
Homo sapiens	c-MAF		Hs04185012_s1
	miR-155		002623
	RNU6B		001093
	ACTB		Hs01060665_g1
	TP53	F	GTTCCGAGAGCTGAATGAGG
		R	TCTGAGTCAGGCCCTTCTGT
	CDKN1A	F	AAGACCATGTGGACCTGT
		R	GGTAGAAATCTGTCATGCTG
	GATA3	F	GCGGGCTCTATCACAAAATG
		R	TCTGACAGTTCGCACAGGAC
	ACTB	F	GATGAGATTGGCATGGCTTT
		R	CACCTTCACCGTTCCAGTTT
ChIP-PCR primer sequence (5' to 3')			
c-MAF promoter		F	TTTTCGGAGCTGTCAATCAG
		R	AAGCCCCTCTGGAAAAACTC
List of oligonucleotide sequence (5' to 3') for CRISPR Cas9 system or genotyping			
gRNA			CAGGAGGATGGCTTCAGAAC
PCR primer		F	GTGTGCACGTTCGAGCTTT
		R	GTCATCCAGTAGTAGTCTTCCAGGT
Sanger sequence primer		R	CAGGTGCGCCTTCTGTTC